

DRAFT

CMS Paper

The content of this note is intended for CMS internal use and distribution only

2011/12/18

Head Id: 91317

Archive Id: 91352:91368

Archive Date: 2011/12/18

Archive Tag: trunk

Search for Heavy Top-like Quark Pair Production in the Dilepton Final State in pp Collisions at $\sqrt{s} = 7$ TeV

The CMS Collaboration

Abstract

The results of a search for pair production of a heavy top-like quark, t' , in the decay mode $t'\bar{t}' \rightarrow bW^+\bar{b}W^- \rightarrow b\ell^+\nu\bar{b}\ell^-\bar{\nu}$ are presented. The search is performed in a data sample corresponding to a total integrated luminosity of 4.68 fb^{-1} of pp collisions at a centre-of-mass energy of 7 TeV, collected by the CMS experiment at the LHC. The observed number of events agrees with the standard model prediction, and no evidence of $t'\bar{t}'$ production is found. Upper limits on the production cross section as a function of t' mass are presented. A t' with a mass below $544 \text{ GeV}/c^2$ is excluded at the 95% C.L.

This box is only visible in draft mode. Please make sure the values below make sense.

PDFAuthor: Yanjun Tu, Jacob Linacre, Frank Wuerthwein
PDFTitle: Search for Heavy Top-like Quark Pair Production in the Dilepton Final State
in pp Collisions at $s=7$ TeV
PDFSubject: CMS
PDFKeywords: CMS, physics, dilepton, top-like, tprime, fourth generation

Please also verify that the abstract does not use any user defined symbols

1 Introduction

Since the discovery of the top quark at the Tevatron, there have been many searches for a possible new generation of fermions. Those searches have not found evidence of new fermions beyond the standard model (SM). However, from a theoretical point of view, the number of generations of fermions is not limited to three. The extension of the generations of fermions may have a significant effect on neutrino physics, flavor physics and Higgs physics. With a fourth generation, indirect bounds on the Higgs boson mass can be relaxed [1, 2], and an additional generation of quarks may possess enough intrinsic matter and anti-matter asymmetry to be relevant for the baryon asymmetry of the Universe [3]. Therefore, there is continued theoretical and experimental interest in such a fourth generation [4]. Previous direct searches restrict the masses of quarks in the fourth generation, t' and b' , to be greater than $350 \text{ GeV}/c^2$ [5, 6], and the indirect search from LEP excludes a fourth generation of light neutrinos [7]. At the LHC, the QCD production cross section of $t'\bar{t}'$ is expected to be significantly larger than that at the Tevatron [8]. This brings us a great opportunity to explore the possibility of new physics with an extended generation of fermions.

We present a search for a heavy top-like quark (t') in the final state $t' \rightarrow bW \rightarrow bl\nu$, using pair production of $t'\bar{t}'$ in pp collisions at a centre-of-mass energy of 7 TeV. This search is well motivated if $M_{t'} < M_{b'}$ or if $M_{t'} > M_{b'}$ and the mass splitting between t' and b' is less than M_W , which is favored by precision electroweak measurements [2, 9]. The dilepton $t'\bar{t}'$ search has a small SM background, and is hence a “clean” environment to search for new physics.

The search uses a data sample corresponding to a total integrated luminosity of 4.68 fb^{-1} collected by the Compact Muon Solenoid (CMS) experiment at the LHC.

2 CMS Detector

The central feature of the CMS apparatus is a superconducting solenoid, 13 m in length and 6 m in diameter, which provides an axial magnetic field of 3.8 T. Within the field volume are several particle detection systems. Charged particle trajectories are measured by silicon pixel and silicon strip trackers, covering $0 \leq \phi \leq 2\pi$ in azimuth and $|\eta| < 2.5$ in pseudorapidity, defined as $\eta = -\log[\tan \theta/2]$, where θ is the polar angle of the trajectory of the particle with respect to the counterclockwise proton beam direction. A crystal electromagnetic calorimeter and a brass/scintillator hadronic calorimeter surround the tracking volume, providing energy measurements of electrons and hadronic jets. Muons are identified and measured in gas-ionization detectors embedded in the steel return yoke outside the solenoid. The detector is nearly hermetic, allowing energy balance measurements in the plane transverse to the beam direction. A two-tier trigger system selects the most interesting pp collision events for use in physics analysis. A more detailed description of the CMS detector can be found elsewhere [10].

3 Event Preselection

The data in this measurement are collected using one of the ee , $e\mu$, or $\mu\mu$ high- p_T double-lepton triggers. Muon candidates are reconstructed with two algorithms, one in which tracks in the silicon detector are matched to consistent signals in the calorimeters and muon system, and another in which a simultaneous fit is performed to hits in the silicon tracker and muon system [11]. Electron candidates are reconstructed starting from a cluster of energy deposits in the electromagnetic calorimeter, which is then matched to hits in the silicon tracker. A selection using electron identification variables based on shower shape and track-cluster matching is ap-

44 plied to the reconstructed candidates [12]. Electron candidates within $\Delta R \equiv \sqrt{\Delta\phi^2 + \Delta\eta^2} < 0.1$
 45 of a muon are rejected to remove candidates due to muon bremsstrahlung and final-state radi-
 46 ation. Both electrons and muons are required to be isolated from other activity in the event. This
 47 is achieved by imposing a maximum allowed value of 0.15 on I_{rel} , an observable defined as the
 48 ratio of the scalar sum of transverse track momenta and transverse calorimeter energy deposits
 49 within a cone of $\Delta R < 0.3$ around the lepton candidate direction at the origin, to the trans-
 50 verse momentum of the candidate. Events selected for the analysis are required to have two
 51 opposite-sign, isolated leptons (e^+e^- , $e^\pm\mu^\mp$, or $\mu^+\mu^-$). Both leptons must have $p_T > 20$ GeV/ c ,
 52 and the electrons (muons) must have $|\eta| < 2.5$ ($|\eta| < 2.4$), and be consistent with originating
 53 from the same interaction vertex. In events with more than two such leptons, the two leptons
 54 with the highest p_T are selected. Events with an e^+e^- or $\mu^+\mu^-$ pair with invariant mass between
 55 76 GeV/ c^2 and 106 GeV/ c^2 or below 12 GeV/ c^2 are removed, in order to suppress Drell-Yan,
 56 $Z/\gamma^* \rightarrow \ell^+\ell^-$ events, as well as low mass dilepton resonances.

57 The jets and the missing transverse energy E_T^{miss} are reconstructed with the Particle Flow tech-
 58 nique [13]. At least two jets with $p_T > 30$ GeV/ c and $|\eta| < 2.5$, separated by $\Delta R > 0.4$ from
 59 leptons passing the analysis selection, are required to be in the event. The anti- k_T clustering
 60 algorithm [14] with $\Delta R = 0.5$ is used for jet clustering. Exactly two of the jets are required to be
 61 consistent with coming from the decay of heavy flavor and be identified as b -jets by the TCHEM
 62 b -tagging algorithm described in [15], which relies on tracks with large impact parameters. The
 63 E_T^{miss} in the event is required to exceed 50 GeV.

64 Signal and background studies are performed using the simulated events generated by the
 65 MADGRAPH 4.4.12 [16] or PYTHIA 6.4.22 [17] event generators. The samples of $t'\bar{t}'$, $t\bar{t}$, Drell-
 66 Yan (DY) with $M_{\ell\ell} > 50$ GeV/ c^2 , di-boson (VV), and single top (tW) events are generated using
 67 MADGRAPH. The samples of Drell-Yan with $M_{\ell\ell} < 50$ GeV/ c^2 are generated using PYTHIA.
 68 They are then simulated using a GEANT4-based model [18] of the CMS detector, and finally
 69 reconstructed and analyzed using the same software as is used to process collision data.

70 Due to the varying LHC luminosity, the mean number of interactions in a single beam cross-
 71 ing increased over the course of data taking to a maximum of ~ 15 near the end of the 2011
 72 data taking period. In the following, the yields of simulated events are weighted such that the
 73 distribution of reconstructed vertices observed in data is simulated. The efficiency for events
 74 containing two leptons satisfying the analysis selection to pass at least one of the double-lepton
 75 triggers is measured to be approximately 100%, 95%, and 90% for ee , $e\mu$, and $\mu\mu$ triggers respec-
 76 tively [19], and corresponding weights are applied to the simulated event yields. In addition,
 77 b -tagging scale factors are applied to simulated events for each jet, due to the difference of b -
 78 tagging efficiencies between data and simulation [15]. The observed and simulated yields after
 79 the above event preselection are listed in Table 1, in which $t\bar{t} \rightarrow \ell^+\ell^-$ and $\text{DY} \rightarrow \ell^+\ell^-$ corre-
 80 spond to dileptonic $t\bar{t}$ and DY decays, including tau leptons. $t\bar{t} \rightarrow \text{fake}$ includes all other $t\bar{t}$
 81 decay modes. The yields are dominated by top-pair production in the dilepton final state, and
 82 reasonable agreement is observed between data and simulation. The expected yields from $t'\bar{t}'$
 83 are also shown for different values of the t' mass, $M_{t'}$.

84 4 Signal Region

85 After preselection, the sample is dominated by SM $t\bar{t}$ events. Since we expect a t' quark to have
 86 a much larger mass than the top quark, we can use variables that are correlated to the decaying
 87 quark mass to help distinguish signal events from $t\bar{t}$ events.

88 The masses of lepton and jet (M_{ljb}), from the t/t' and \bar{t}/\bar{t}' decays, are chosen for this purpose.

Table 1: The observed and simulated yields after the preselection described in the text, for an integrated luminosity of 4.68 fb^{-1} . Uncertainties are statistical only.

Sample	ee	$\mu\mu$	$e\mu$	all
$t'\bar{t}'$, $M_{t'} = 400 \text{ GeV}/c^2$	9.58 ± 0.82	12.51 ± 0.92	26.52 ± 1.37	48.61 ± 1.85
$t'\bar{t}'$, $M_{t'} = 500 \text{ GeV}/c^2$	2.69 ± 0.22	2.97 ± 0.22	6.02 ± 0.32	11.67 ± 0.44
$t'\bar{t}'$, $M_{t'} = 600 \text{ GeV}/c^2$	0.81 ± 0.07	0.92 ± 0.07	1.98 ± 0.11	3.72 ± 0.15
$t\bar{t} \rightarrow \ell^+\ell^-$	447.93 ± 10.18	563.43 ± 11.01	1350.76 ± 17.38	2362.12 ± 22.95
$t\bar{t} \rightarrow \text{fake}$	6.62 ± 1.23	0.41 ± 0.25	9.68 ± 1.48	16.71 ± 1.94
W + jets	0	0	0	0
DY $\rightarrow \ell^+\ell^-$	2.63 ± 1.33	1.48 ± 0.86	0.52 ± 0.44	4.63 ± 1.64
Di-boson	0.48 ± 0.10	1.00 ± 0.14	1.76 ± 0.22	3.24 ± 0.27
Single top	14.08 ± 0.88	17.55 ± 0.95	42.30 ± 1.53	73.93 ± 2.00
Total Background	471.74 ± 10.38	583.86 ± 11.09	1405.03 ± 17.51	2460.64 ± 23.18
Data	510	615	1487	2612

89 At generator level, all $t\bar{t}$ events have M_{lb} less than $\sqrt{M_t^2 - M_W^2}$, while most of the $t'\bar{t}'$ events
 90 have M_{lb} larger than that value. At reconstruction level, there are two ways to combine the two
 91 leptons and two b jets in each event, giving four possible values of M_{lb} . The minimum value of
 92 the four masses (M_{lb}^{\min}) is found to be a good variable to distinguish the signal events from $t\bar{t}$
 93 events.

94 Following these observations, the signal region is defined by adding the requirement of the
 95 minimum mass of lepton and jet pairs to the preselection: $M_{lb}^{\min} > 170 \text{ GeV}/c^2$. This additional
 96 selection reduces the expected number of $t\bar{t}$ events by four orders of magnitude compared to
 97 the preselection prediction of Table 1. The simulated yields of $t'\bar{t}'$ events are typically reduced
 98 by 50%, and are given for different values of $M_{t'}$ in Table 2.

Table 2: The expected yields of $t'\bar{t}'$ events in the signal region for different values of $M_{t'}$, for an integrated luminosity of 4.68 fb^{-1} . Uncertainties are statistical only.

Sample	ee	$\mu\mu$	$e\mu$	all
$t'\bar{t}'$, $M_{t'} = 400 \text{ GeV}/c^2$	3.13 ± 0.46	4.91 ± 0.57	10.01 ± 0.83	18.04 ± 1.11
$t'\bar{t}'$, $M_{t'} = 500 \text{ GeV}/c^2$	1.30 ± 0.15	1.74 ± 0.17	3.00 ± 0.22	6.04 ± 0.32
$t'\bar{t}'$, $M_{t'} = 600 \text{ GeV}/c^2$	0.51 ± 0.06	0.54 ± 0.06	1.20 ± 0.08	2.24 ± 0.12

99 5 Background Estimation

100 One of the main causes of background events appearing in the signal region is the misidentifica-
 101 tion of b jets and leptons. We define a misidentified lepton as a lepton candidate not originating
 102 from an electroweak decay, such as a lepton from semileptonic b or c decays, a muon decay-in-
 103 flight, a pion misidentified as an electron, or an unidentified photon conversion. Misidentified
 104 b jets are referred to as “mistags”, and occur when a non- b jet is mistakenly b -tagged.

105 The background events in the signal region can be classified into the following categories:

- 106 • Category I: events with mistagged b (s) and real leptons
- 107 • Category II: events with misidentified lepton(s) and real bs
- 108 • Category III: events with 2 real bs and 2 real leptons

- Category IV: events with mistagged b (s) and misidentified lepton(s).

To predict the number of events with mistagged b (s) (Category I), we use control regions in data where events pass all selection requirements except the number of b -tagged jets. The number of background events with one mistag, $N_{1\text{-mistag}}$, is estimated from events with 1 b -tag, where each event is weighted based on the mistag rate(s) m_i for the untagged jet(s) in the event, which gives the probability for such a non- b jet to be b -tagged. Where there are no untagged jets passing selection the event weight is zero, and for each untagged jet i passing selection the event weight is increased by $m_i/(1 - m_i)$. We then make a similar calculation using events with 0 b -tags to estimate the number events with 2 mistags, $N_{2\text{-mistags}}$. This time a weight of $\frac{m_i}{1-m_i} \times \frac{m_j}{1-m_j}$ is used, where m_i and m_j are the mistag rates for two untagged jets. The final prediction is obtained from $N_{\text{mistags}} = N_{1\text{-mistag}} - N_{2\text{-mistags}}$, which takes into account that $N_{2\text{-mistags}}$ is counted twice in $N_{1\text{-mistag}}$. The performance of the method is checked using simulated events, and an under-prediction of up to 50% is observed. Thus, we assign a 100% systematic uncertainty to the prediction. Finally, we apply the method to predict the number of events with mistags in the signal region in data. The result is $N_{\text{mistags}} = 0.74 \pm 0.27 \pm 0.74$, where the first uncertainty is statistical and the second uncertainty is the 100% systematic uncertainty assigned to the method.

The background from events with misidentified leptons (Category II) is predicted based on the number of events with a candidate lepton that can only pass loosened selection criteria [20]. Using a measurement of the fraction of such ‘‘loose’’ leptons that go on to pass our selection cuts, we can estimate the number of misidentified leptons in our event samples. However, there are no events in data where one or more of the lepton candidates passes only the loosened selection criteria, resulting in a prediction of $0.0_{-0.0}^{+0.4}$ events where the upper uncertainty corresponds to what we would have calculated had we found one such event.

We rely on simulation to predict the number of events with no misidentified b s or leptons (Category III). Selecting only events where both b s and leptons are well matched to corresponding particles at generator level, the resulting prediction is 0.93 ± 0.65 where the uncertainty is statistical only.

The contribution of events from Category IV is assumed to be negligible. It is covered by both the Category I and Category II predictions, but since the Category II prediction is zero no double-counting can have occurred.

6 Systematic Uncertainties

The systematic uncertainty of the signal acceptance is dominated by a 10% uncertainty [15] on the b -tagging efficiency for high- p_T b -jets. Other uncertainties are assessed on the trigger efficiency (2%) [19], lepton selection (2%) [19], and jet and E_T^{miss} energy scale (8%) [21]. These four sources combine to a 22% relative uncertainty on the signal Acceptance \times Efficiency, and there is a further 4.5% uncertainty on the luminosity [22].

The systematic uncertainty of the background estimate is dominated by the uncertainty on the data driven estimate of events with mistagged b jets (100%), and the lack of selected events in the loose-lepton control region. The systematic uncertainties on these sources of background are included in the summary of background predictions in Table 3.

7 Results and Conclusions

We expect 1.67 ± 1.10 events from SM background processes and observe one event in the $e\mu$ channel. We thus see no evidence for an excess of events above SM expectations. A summary of the observed and predicted yields is presented in Table 3.

The simulated distribution of M_{lb}^{\min} from SM background processes is compared to the data in Figure 1, where the expected distribution for a $t'\bar{t}'$ signal with $M_{t'} = 450 \text{ GeV}/c^2$ is also shown. The simulated background yields in the signal region are scaled so that they match the yields estimated from control regions in data given in Table 3, and outside the signal region the simulated background yields are taken without rescaling.

Table 3: Summary of the observed and predicted yields. Uncertainties include both statistical and systematic errors, apart from Category III where the uncertainty is statistical only.

Sample	Yield
Category I (data-driven)	0.74 ± 0.79
Category II (data-driven)	$0^{+0.4}_{-0.0}$
Category III (simulated)	0.93 ± 0.65
Total prediction	1.67 ± 1.10
Data	1

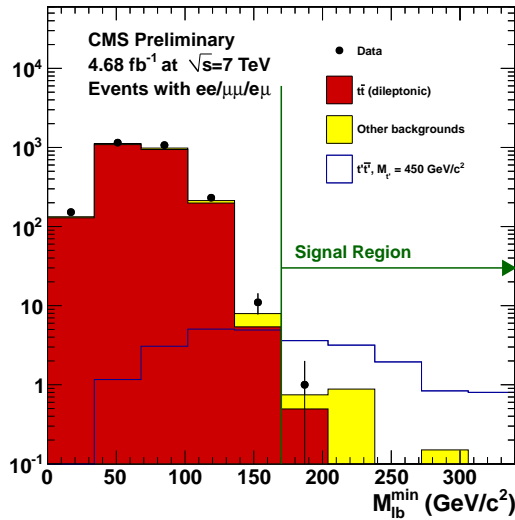


Figure 1: Comparison of data and the simulated background for M_{lb}^{\min} . The signal region is defined by $M_{lb}^{\min} > 170 \text{ GeV}/c^2$. The simulated background yields in the signal region are scaled so that they match the yields estimated from control regions in data given in Table 3, and outside the signal region the simulated background yields are taken without rescaling. One data event is observed in the signal region. The expected distribution for a $t'\bar{t}'$ signal is also shown for $M_{t'} = 450 \text{ GeV}/c^2$.

Since no excess beyond the SM background is found, 95% C.L. upper limits on the production cross section of $t'\bar{t}'$ as a function of t' mass are set, using the CL_s method [23, 24].

The limit calculation is based on the information provided by the observed event count combined with the values and the uncertainties of the luminosity measurement, the background prediction, and the fraction of all $t'\bar{t}'$ events expected to be selected. This fraction is

164 the Efficiency \times Acceptance \times Branching Ratio for simulated signal events, and is given in
 165 Table 4 for different values of $M_{t'}$.

166 The calculated limits are shown in Figure 2 and Table 5. As a conclusion, the expected and
 167 observed 95% C.L. lower bounds on the t' mass are 537 GeV/c^2 and 544 GeV/c^2 respectively
 168 from the analysis of a data sample corresponding to an integrated luminosity of 4.68 fb^{-1} .

Table 4: Efficiency \times Acceptance \times Branching Ratio in simulated events for different t' masses. Each value has a relative uncertainty of 22%.

Sample	Eff \times Acc \times BR
$t'\bar{t}'$, $M_{t'} = 350 \text{ GeV}/c^2$	0.15%
$t'\bar{t}'$, $M_{t'} = 400 \text{ GeV}/c^2$	0.27%
$t'\bar{t}'$, $M_{t'} = 450 \text{ GeV}/c^2$	0.33%
$t'\bar{t}'$, $M_{t'} = 500 \text{ GeV}/c^2$	0.39%
$t'\bar{t}'$, $M_{t'} = 550 \text{ GeV}/c^2$	0.46%
$t'\bar{t}'$, $M_{t'} = 600 \text{ GeV}/c^2$	0.52%

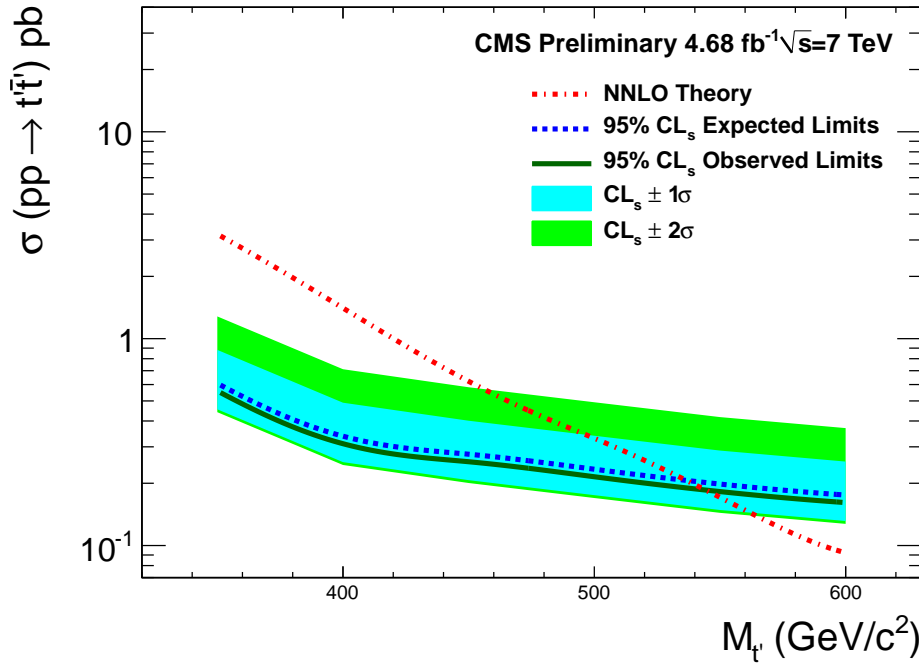


Figure 2: The 95% C.L. upper limits on the production cross section of $t'\bar{t}'$ as a function of t' mass are shown. The expected 95% C.L. lower bound on $M_{t'}$ is 537 GeV/c^2 and the observed 95% C.L. lower bound on $M_{t'}$ is 544 GeV/c^2 .

169 References

- 170 [1] P. Q. Hung and M. Sher, "Experimental constraints on fourth generation quark masses",
 171 *Phys. Rev. D* **77** (Feb, 2008) 037302. doi:10.1103/PhysRevD.77.037302.
- 172 [2] G. D. Kribs, T. Plehn, M. Spannowsky et al., "Four generations and Higgs physics", *Phys.*
 173 *Rev. D* **76** (Oct, 2007) 075016. doi:10.1103/PhysRevD.76.075016.

Table 5: The expected NNLO theoretical cross section of $t'\bar{t}'$ production [25] and the 95% C.L. upper limits on the production cross section of $t'\bar{t}'$.

$M_{t'}$	350 GeV/ c^2	400 GeV/ c^2	450 GeV/ c^2	500 GeV/ c^2	550 GeV/ c^2	600 GeV/ c^2
Theory (pb)	3.200	1.406	0.622	0.330	0.171	0.092
Expected (pb)	0.608	0.338	0.276	0.234	0.198	0.175
Observed (pb)	0.559	0.311	0.254	0.215	0.182	0.161

- 174 [3] W.-S. Hou, “CP Violation and Baryogenesis from New Heavy Quarks”, *Chin. J. Phys.* **47**
175 (2009) 134, arXiv:0803.1234.
- 176 [4] B. Holdom et al., “Four Statements about the Fourth Generation”, *PMC Phys.* **A3** (2009)
177 4, arXiv:0904.4698. doi:10.1186/1754-0410-3-4.
- 178 [5] The CDF Collaboration, “Search for Heavy Top $t' \rightarrow Wq$ in Lepton Plus Jets Events in 4.6
179 fb^{-1} ”, *CDF public conference note CDF/PUB/TOP/PUBLIC/10110 (unpublished)* (2010).
- 180 [6] The CDF Collaboration, “Search for heavy bottom-like quarks decaying to an electron or
181 muon and jets in $p\bar{p}$ collisions at $\sqrt{s} = 1.96 \text{ TeV}$ ”, *Phys. Rev. Lett.* **106** (2011) 141803,
182 arXiv:1101.5728. doi:10.1103/PhysRevLett.106.141803.
- 183 [7] D. Decamp et al., “Determination of the number of light neutrino species”, *Phys. Lett. B*
184 **231** (1989) 519.
- 185 [8] E. L. Berger and Q.-H. Cao, “Next-to-Leading Order Cross Sections for New Heavy
186 Fermion Production at Hadron Colliders”, *Phys. Rev.* **D81** (2010) 035006,
187 arXiv:0909.3555. doi:10.1103/PhysRevD.81.035006.
- 188 [9] O. Eberhardt, A. Lenz, and J. Rohrwild, “Less space for a new family of fermions”, *Phys.*
189 *Rev.* **D82** (2010) 095006, arXiv:1005.3505.
190 doi:10.1103/PhysRevD.82.095006.
- 191 [10] CMS Collaboration, “The CMS experiment at the CERN LHC”, *JINST* **3** (2008) S08004.
- 192 [11] CMS Collaboration, “Performance of muon identification in pp collisions at $\sqrt{s} = 7 \text{ TeV}$ ”,
193 *CMS Physics Analysis Summary CMS-PAS-MUO-10-002* (2010).
- 194 [12] CMS Collaboration, “Electron reconstruction and identification at $\sqrt{s}=7 \text{ TeV}$ ”, *CMS*
195 *Physics Analysis Summary CMS-PAS-EGM-10-004* (2010).
- 196 [13] CMS Collaboration, “Commissioning of the Particle–Flow reconstruction in
197 Minimum–Bias and Jet Events from pp Collisions at 7 TeV”, *CMS Physics Analysis*
198 *Summary CMS-PAS-PFT-10-002* (2010).
- 199 [14] M. Cacciari, G. Salam, and G. Soyez, “The anti- k_T jet clustering algorithm”, *Journal of*
200 *High Energy Physics* **2008** (2008), no. 04, 063.
- 201 [15] CMS Collaboration, “Commissioning of b-jet identification with pp collisions at
202 $\sqrt{s} = 7 \text{ TeV}$ ”, *CMS Physics Analysis Summary CMS-PAS-BTV-10-001* (2010).
- 203 [16] J. Alwall et al., “MadGraph/MadEvent v4: The New Web Generation”, *JPHYS* **31** (2005)
204 N9–N20.

- 205 [17] T. Sjöstrand, S. Mrenna, and P. Skands, “PYTHIA 6.4 Physics and Manual”, *JHEP* **05**
206 (2006) 026.
- 207 [18] GEANT 4 Collaboration, “GEANT4 – a simulation toolkit”, *Nucl. Instr. and Methods A*
208 **506** (2003) 250–303.
- 209 [19] CMS Collaboration, “Search for Physics Beyond the Standard Model in Opposite-Sign
210 Dilepton Events at $\sqrt{s} = 7$ TeV”, *CMS Physics Analysis Summary* **CMS-PAS-SUS-11-011**
211 (2011).
- 212 [20] CMS Collaboration, “Search for new physics with same-sign isolated dilepton events
213 with jets and missing transverse energy at the LHC”, [arXiv:1104.3168v1](https://arxiv.org/abs/1104.3168v1).
- 214 [21] CMS Collaboration, “Determination of the Jet Energy Scale in CMS with pp Collisions at
215 $\sqrt{s} = 7$ TeV”, *CMS Physics Analysis Summary* **CMS-PAS-JME-10-010** (2010).
- 216 [22] CMS Collaboration, “Measurement of CMS Luminosity”, *CMS Physics Analysis Summary*
217 **CMS-PAS-EWK-10-004** (2010).
- 218 [23] T. Junk, “Confidence level computation for combining searches with small statistics”,
219 *Nucl. Instrum. Meth.* **362** (1999) 435.
- 220 [24] A. L. Read, “Presentation of search results: The CL_s technique”, *J. Phys. G28* **364** (2002)
221 2693.
- 222 [25] M. A. et al., “HATHOR, HAdronic Top and Heavy quarks cross section calculator”,
223 *Comput. Phys. Commun.* **182** (2011) 1034.